

Thermal properties of layered transition-metal dichalcogenides at charge-density-wave transitions*

J. M. E. Harper

IBM Thomas J. Watson Research Center, Yorktown Heights, New York 10598

T. H. Geballe

Department of Applied Physics, Stanford University, Stanford, California 94305

F. J. DiSalvo

Bell Laboratories, Murray Hill, New Jersey 07974

(Received 12 November 1976)

The heat capacity and resistivity at the charge-density-wave (CDW) transitions of several layered transition-metal dichalcogenides are presented. The magnitude of the thermal and resistive anomalies in the $2H$ polytypes indicates only a small fraction of the Fermi surface is involved in the CDW distortion. The transition from the normal to the incommensurate CDW state at T_0 is second order, while the transition to the commensurate CDW state at T_d is first order. However, the heat capacity anomaly at T_0 , especially in $2H$ -TaSe₂, does not show the simple BCS-like jump expected from Landau models, rather a peak in the heat capacity occurs at T_0 .

I. INTRODUCTION

Charge density waves (CDW) in the layered transition-metal dichalcogenides have been observed in electron-diffraction studies by Wilson *et al.* and Williams *et al.*¹ and in neutron diffraction studies by Moncton *et al.*² The driving force for the CDW in the $1T$ polytypes is thought to originate in the coupling of near-parallel segments of the Fermi surface.¹ In the $2H$ polytypes a somewhat different mechanism has been proposed by Rice *et al.*³ in which coupling occurs between saddle points in the band structure close to the Fermi surface. These different mechanisms may account for the difference in the onset temperatures (T_0) of the $1T$ and $2H$ polytypes and also for their quite different transport properties. Phenomenological Landau theories have been proposed by McMillan⁴ and by Moncton² which predict thermal anomalies at the transition from normal metal to incommensurate charge density wave (ICDW) at T_0 and from incommensurate to commensurate charge density wave (CCDW) at T_d .

In this paper we present the thermal properties at the CDW transitions in some of these materials. Both absolute and relative heat-capacity measurements were made using a newly developed small-sample calorimeter.⁵ The materials studied were $2H$ -NbSe₂, $2H$ -TaS₂, $2H$ -TaSe₂, $4Hb$ -TaS₂, $4Hb$ -TaSe₂, and $1T$ -VSe₂.

The magnitude of the thermal anomalies suggests that a small fraction of the Fermi surface participates in the CDW distortion in the $2H$ polytypes. Also the effect of the CDW on superconductivity in

$2H$ -NbSe₂ is shown to be small. The entropy of transformation in the $2H$ polytypes is more than an order of magnitude less than in the $1T$ polytypes, consistent with the proposed difference in driving force.¹ In $4Hb$ -TaS₂ thermal anomalies are observed at the different CDW transition which occur independently in the octahedral and trigonal-prismatic layers.^{1,6} In $4Hb$ -TaSe₂ and $1T$ -VSe₂ no thermal anomalies could be observed below 150 K, although they were anticipated from the transport properties.^{1,7}

In Sec. IIB the methods of heat-capacity measurements will be described. The results will be given in Sec. III for each material separately, and in Sec. IV we give a comparative discussion.

II. EXPERIMENTAL METHOD

A. Sample preparation

The crystals were prepared using vapor transport techniques described elsewhere⁸ and were typically 10–20 mg in size. The crystal of $1T$ -VSe₂ was 3 mg in size, and was supplied by A. H. Thompson of Exxon Research and Engineering Co., Linden, N. J.

B. Heat-capacity measurements

Heat-capacity measurements were made using a small-sample calorimeter designed to give both accurate absolute heat-capacity measurements and high-resolution relative heat-capacity measurements over the temperature range 4 to 150 K. A detailed description of the calorimeter is given

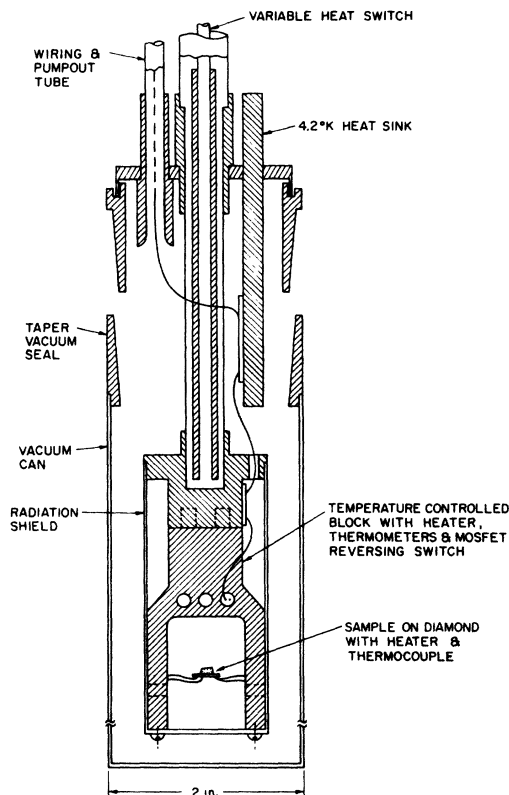


FIG. 1. Small sample calorimeter.

in Ref. 5.

Figure 1 shows the sample mounted with thermally conducting grease⁹ on a diamond substrate, which carries a resistive heater and a Au-0.07-at.-% Fe vs cromel thermocouple (0.003-in. diam) to measure the sample temperature. The thermocouple is referenced to a temperature-controlled copper block, which carries a calibrated germanium resistance thermometer¹⁰ and silicon diode thermometer¹¹ for absolute-temperature measurement. To allow operation over a wide temperature range, a variable heat switch was designed to vary the thermal link between the reference block and helium reservoir. The heat switch consists of a movable vertical tube inside the thin-walled stainless-steel support tube to the block. This tube contains a vacuum space isolated from the sample region. By raising or lowering the tube and by varying the pressure of helium gas inside the vacuum space, the thermal link may be varied by a factor of 10. The helium gas does not enter the sample region, precluding problems due to gas absorption on the surface of the sample.

Figure 2 shows the measurement system in schematic form. This apparatus incorporates the on-line computer system developed by Schwall

*et al.*¹² for automated small-sample calorimetry, which uses a signal averaging computer and mini-computer to analyze data and control the experiment. The thermocouple signal measuring the sample temperature is converted to an ac signal by a MOSFET (metal-oxide-semiconductor field-effect transistor) reversing switch operating at 1 kHz, and synchronously detected with a lock-in amplifier.¹³ Modulating the signal at low temperatures minimizes the effect of thermal emf's in the lead wires and reduces the noise level to about 2 nV corresponding to a temperature resolution of 0.1 mK.

The absolute heat-capacity measurements presented here were made using the relaxation method¹⁴ in which the temperature response of the sample to a step change in heater power is analyzed to yield a time-constant proportional to the heat capacity of sample plus addendum. For a 10-mg metal sample the ratio of addendum to sample heat capacity is typically less than 0.5 over the range 4 to 90 K. Typical resolution for a 10-mg metal sample is $\pm 2\%$ – 3% absolute heat capacity in the temperature range 4 to 90 K and $\pm 5\%$ from 90 to 150 K.

Greater resolution of structure in the heat capacity is obtained using a relative measurement. In the sweep method used in these measurements⁵ the block temperature is swept linearly with time (heating or cooling) and the temperature difference $\Delta T = T_{\text{sample}} - T_{\text{block}}$ is monitored. ΔT is proportional to the heat capacity of sample plus addendum, giving a continuous readout of relative heat capacity. This method is ideal for sweeping over a wide temperature range to locate anomalies in the heat capacity and is also suited to detailed examination of the shape of a heat-capacity anomaly. It has been found in this work that the sweep method can be successfully used with thermal time constants typical of the relaxation method and that relative changes of the heat capacity of $\pm 0.1\%$ can be observed.

Thus, it is possible in the same apparatus to combine accurate absolute measurements using

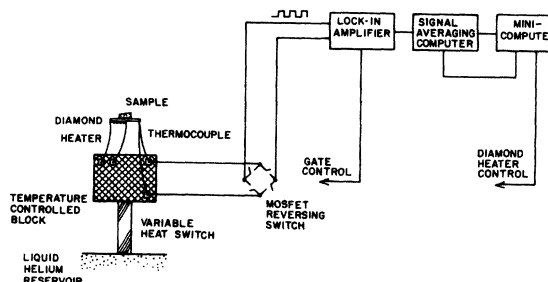


FIG. 2. Schematic diagram of small-sample calorimeter.

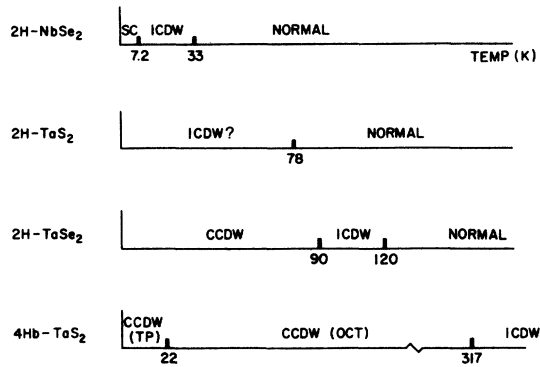


FIG. 3. Charge-density-wave transitions studied.

the relaxation method with relative measurements using the sweep method, both operating over a wide temperature range. For the materials studied here, absolute heat-capacity measurements were made using the relaxation method from 5 to 15 K to determine the low-temperature coefficients of the heat capacity. Further absolute measurements were made in the region of the CDW transitions to calibrate the sweep method. Detailed measurements using the sweep method were then made to determine the shape of the thermal anomalies, measure the heat of transformation, and examine for evidence of hysteresis. Simultaneous resistivity measurements were performed in most cases using the standard four-lead method with an ac current of typically 1 mA at 27.5 Hz.

III. RESULTS

Figure 3 shows a schematic diagram of the temperature regions of stability of the CDW phases studied here. The results for each sample are

summarized in Table I, in which the following information is listed: (i) T_c is the superconducting transition temperature; (ii) γ is the coefficient of the linear term in the low-temperature heat capacity; (iii) β is the coefficient of the cubic term in the low-temperature heat capacity; (iv) Θ_D is the Debye temperature obtained from β , assuming three atoms per molar unit (another common convention for Θ_D treats the three atoms as one unit, giving values of Θ_D smaller by a factor of 0.69 than the values given here); (v) T_0 is the onset temperature of the CDW transition; (vi) "order" stands for the thermodynamic order of the transition, first or second; (vii) $\Delta C/C$ is the fractional height of the heat-capacity anomaly in % of the absolute heat capacity at T_0 ; (viii) $\Delta\rho/\rho$ is the fractional height of the resistivity anomaly in % of the resistivity at T_0 ; (ix) ΔH is the integrated heat of transformation of the transition (Uncertainty in establishing the background heat capacity limits the accuracy of ΔH to 10%–20%.); (x) ΔS is the entropy of transition, approximately equal to $\Delta H/T_0$.

The values of γ and β measured here agree to within 10%–15% with those obtained by Schwall¹⁵ ($2H-NbSe_2$, $2H-TaS_2$), Revelli¹⁶ ($2H-TaSe_2$), and Meyer¹⁷ ($4Hb-TaS_2$). The difference in Θ_D between the S and Se compounds is explained by the mass difference. $2H-TaS_2$ becomes superconducting at 0.8 K,¹ and a variety of intercalation and doping schemes¹⁸ have been found to raise T_c to 3–4 K. These effects have been correlated with the suppression of the CDW transition at 78 K.¹⁹

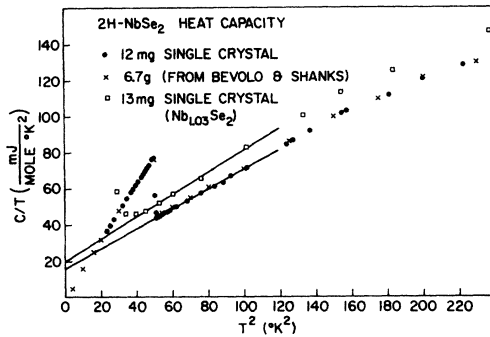
A. $2H-NbSe_2$

$2H-NbSe_2$ is unique among these materials in that it has a relatively high superconducting transition temperature ($T_c = 7.2$ K). Thus, the connection be-

TABLE I. Charge-density-wave transitions.

Material	T_c (K)	γ mJ mole K ²	β mJ mole K ⁴	Θ_D (K)	T_0 (K)	Order	$\Delta C/C$ (%)	$\Delta\rho/\rho$ (%)	ΔH (J/mole)	ΔS (J/mole K)
$2H-NbSe_2$	7.2	16.0	0.55	222	33.5	Second	6.5	3	1.9	0.059
$2H-TaS_2$	0.8 (Ref. 1)	7.5	0.44	236	78.0	Second	5.6	0.3 ^a	4.0	0.052
$2H-TaSe_2$	0.15 (Ref. 1)	4.5	0.71	202	121 90	Second First	22 <0.1	1.5 <0.1 ^c	55 ...	0.460 ...
$4Hb-TaS_2$	<1.1 (Ref. 1)	3.0	0.45	234	317 22	First First ^b ... ^b	440.0 1.3	1.40 0.059
$4Hb-TaSe_2$	<1.1 (Ref. 1)	4.5	0.83	192	≈75		No anomaly observed			
$1T-VSe_2$	<1.1 (Ref. 7)	110 ≈80		No anomalies observed			

^a Tidman (Ref. 24) has observed $\Delta\rho/\rho = 1.5\%$.^b These samples not measured. See Fig. 12.^c Other samples show $\Delta\rho/\rho \approx 1\%$ (Refs. 23 and 32).

FIG. 4. 2H-NbSe₂ heat capacity up to 15 K.

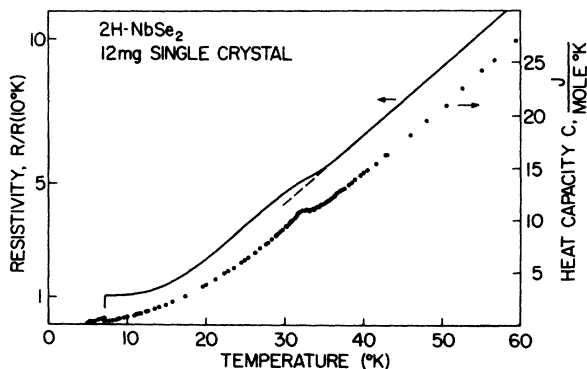
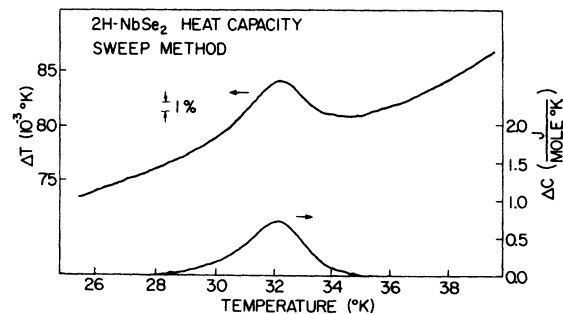
tween superconductivity and the CDW instability is of interest.²⁰ The results given here, however, show that the occurrence of the CDW has little effect on the superconducting properties of the material. The results for 2H-NbSe₂ have been previously published in Ref. 21, and the values of γ and β are in close agreement with those measured by Schwall.¹⁵ In Fig. 4 the low-temperature heat capacity is plotted, showing the sharp superconducting transition for the 12-mg crystal measured here. Also plotted are some of the data for a 6.7-g sample of polycrystalline NbSe₂ measured by Bevolo and Shanks²² in an attempt to observe a heat capacity anomaly associated with the CDW transition. No anomaly associated with the CDW transition was found by Bevolo and Shanks, the transition having been apparently suppressed by different sample preparation techniques¹⁸ or by the application of pressure in preparing the sample for the calorimeter.¹ However, the heat capacity of the transforming crystal is identical to within about 1% to that of the nontransforming sample in this temperature range, indicating little effect due to the onset of the CDW. More recent measure-

ments by Bevolo and Shanks²² showed the presence of a heat-capacity anomaly in NbSe₂ in agreement with the results presented here. Also shown in Fig. 4 are the results for a sample with excess Nb, measured to observe the effect of suppressing the CDW transition with impurities. The superconducting transition was slightly lowered (to 6.5 K onset in susceptibility) and the anomaly at the CDW transition almost entirely suppressed.

Figure 5 shows the heat capacity and resistivity up to 60 K, indicating the anomalies at 33.5 K. Sweep measurements (Fig. 6) were made to study the shape of the anomaly. The excess heat capacity ΔC obtained by subtracting the background is also shown in Fig. 6. The anomaly ($\Delta C/C = 6.5\%$) is quite rounded and reproducible upon heating and cooling, with no evidence of hysteresis. The transition appears to be second order, with no evidence of a first-order component. The onset temperature and second-order character are in excellent agreement with the neutron-scattering measurements of Moncton *et al.*³ and with elastic constant measurements by Barmatz²³ which show a softening of the Young's modulus at the transition. The proportionality between the heat capacity and Young's modulus anomalies predicts a pressure dependence of the transition temperature of $dT_0/dp < -1$ K/kbar. This is in agreement with recent measurements by Chu *et al.*²⁰ and by Berrthier *et al.*²⁰ who both found $dT_0/dp = -0.3$ K/kbar.

The value of γ and the resistivity do not change appreciably when the CDW is present, suggesting that the CDW transition does not involve a large fraction of the Fermi surface. The magnitude of ΔH , the enthalpy of transformation, reflects the weak nature of the transition, being about $\frac{1}{100}$ the magnitude involved in the higher temperature transitions in the 1T polytypes.¹

Further other bulk properties such as magnetic susceptibility show no change ($\pm 1\%$) near T_0 .¹ It seems clear that only a few percent or less of the

FIG. 5. 2H-NbSe₂ heat capacity and resistivity up to 60 K.FIG. 6. 2H-NbSe₂ heat capacity at CDW transition—sweep method.

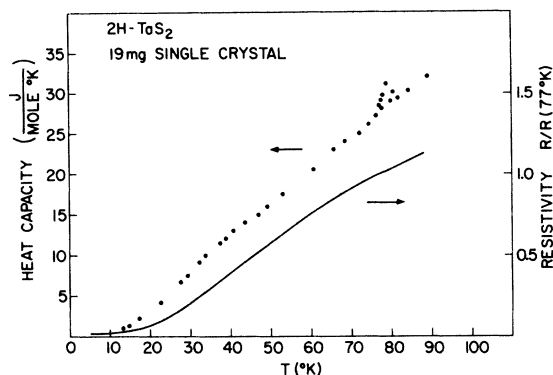


FIG. 7. $2H\text{-TaS}_2$ heat capacity and resistivity up to 90 K.

Fermi surface (or density of states at the Fermi level) is involved in this transition.

It the simplest models,² the gaps produced at the Fermi surface will be BCS-like. Consequently, we would expect a discontinuous increase in the heat capacity at T_0 , with $\Delta C = C_{CDW} - C_N$ being non-zero down to $T=0$ K. Rather we observe a small bump centered at T_0 . Since an adequate model for the shape of this anomaly does not exist, we can not more accurately assess the total number of states at the Fermi level involved in this transition.

B. $2H\text{-TaS}_2$

Figure 7 shows the heat capacity and resistivity of $2H\text{-TaS}_2$ up to 90 K illustrating the normal to ICDW transition at 78 K. The scatter in the absolute measurements of heat capacity at 78 K is due to poor temperature control in the immediate vicinity of liquid-nitrogen temperature. The transition is, however, smooth and reproducible ($\Delta C/C = 5.6\%$) as shown in the sweep trace of Fig. 8.

The shape of the transition remained unchanged as the sweep rate was varied from 20 to 300 sec/K and no hysteresis was observed, thus the transition appears second order. Tidman²⁴ observed a sharp jump in the resistivity ($\Delta\rho/\rho = 1.5\%$) at 75.3 K and suggested this transition is first order. However, in the sample measured here we found no evidence of a first-order component to the transition. In this sample the resistivity anomaly is small ($\Delta\rho/\rho = 0.3\%$). The resistivity ratio $\rho(77\text{ K})/\rho(5\text{ K})$ is 55, whereas Tidman reports a ratio of 22. Thus, sample quality does not appear to account for the difference in size of the resistivity anomaly.

The entropy of transition ($\Delta S = 0.052\text{ J/mole K}$) is close to the value for $2H\text{-NbSe}_2$ and in all re-

spects these two transitions appear similar with the only difference being the transition temperature. Heat-capacity and resistivity measurements of the CDW transition in $2H\text{-TaS}_2$ have also been made by Craven²⁵ who finds similar anomalies but with a sharper peak in ΔC so that $\Delta C/C$ is about 15%. The transition temperature measured by Craven (78 K) agrees with the present measurement. The pressure dependence of the transition has recently been studied by Delaplace *et al.*²⁶

The thermodynamic data are not too dissimilar from that of $2H\text{-NbSe}_2$, so again we might estimate that the fraction of Fermi surface involved in the transitions is only a few percent. However, the magnetic susceptibility decreases by approximately 15% below T_0 suggesting that a somewhat larger fraction (at least of the density of states at the Fermi level) is involved.

C. $2H\text{-TaSe}_2$

$2H\text{-TaSe}_2$ provides the opportunity to study both the normal to ICDW transition at $T_0 = 120\text{ K}$ and the ICDW to CCDW transition at $T_d = 90\text{ K}$. From elastic-constant measurements by Barmatz,²³ it was expected that the major thermal anomaly would be found at 120 K; however, the opposite was found. The heat-capacity anomaly at 120 K is very pronounced, while the 90-K transition is barely discernible. Figure 9 shows the heat capacity and resistivity up to 160 K, and Fig. 10 the absolute heat capacity in the region of 120 K. In Fig. 11 the anomalies at 120 and 90 K are compared, the latter visible only as slight kinks in the resistivity and sweep heat capacity (with hysteresis of several degrees). These measurements were made on the same sample studied by Barmatz to eliminate

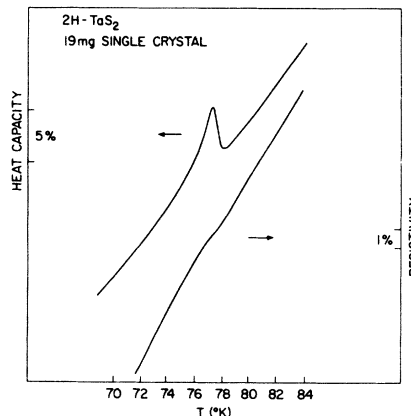


FIG. 8. $2H\text{-TaS}_2$ heat capacity (sweep method) and resistivity at CDW transition.

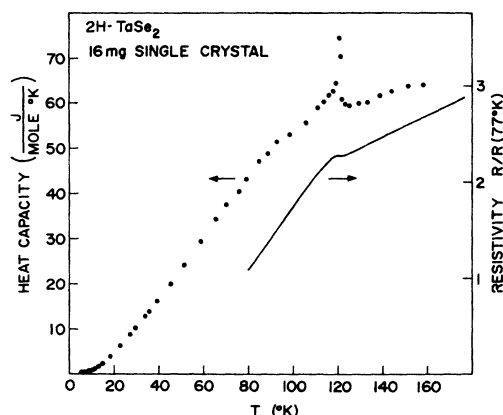


FIG. 9. $2H$ - $TaSe_2$ heat capacity and resistivity up to 160 K.

sample-dependent effects. The resistance ratio of this sample is $\rho(300\text{ K})/\rho(4\text{ K})=74$. A further analysis of the thermal and elastic properties of $2H$ - $TaSe_2$ is given in Ref. 27. Detailed heat-capacity measurements of these transitions have recently been made by Craven²⁵ in samples with resistance ratios of about 300. At the ICDW to CCDW transition the magnitude and temperature of the thermal anomaly are found to be sample dependent. At the normal to ICDW transition the sharpness of the thermal anomaly is found to vary between samples, while the transition temperature and heat of transformation ΔH remain constant.

Infrared reflectivity measurements by Barker *et al.*²⁸ on $2H$ - $TaSe_2$ have revealed extra structure near 0.3 eV upon cooling below 120 K. The oscillator strength in the absorption anomaly gives an estimate of the fraction of Fermi surface involved being on the order of 1% or less. However, the exact interpretation of this structure is not totally clear, in particular it may not be due to a simple

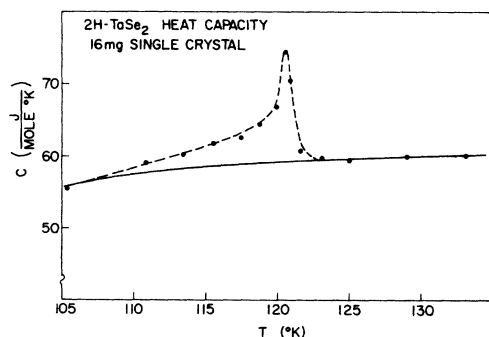


FIG. 10. $2H$ - $TaSe_2$ heat capacity at CDW transition—relaxation method. The dashed line follows the data and the full line is an extrapolation from above the transition.

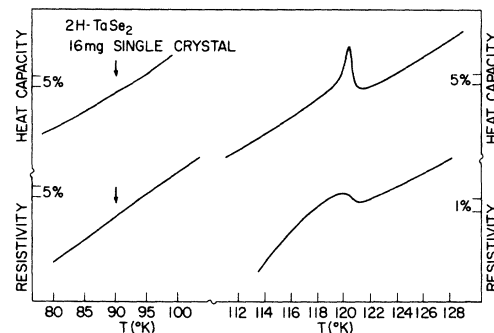


FIG. 11. $2H$ - $TaSe_2$ heat capacity (sweep method) and resistivity at CDW transitions.

gap in the band structure.

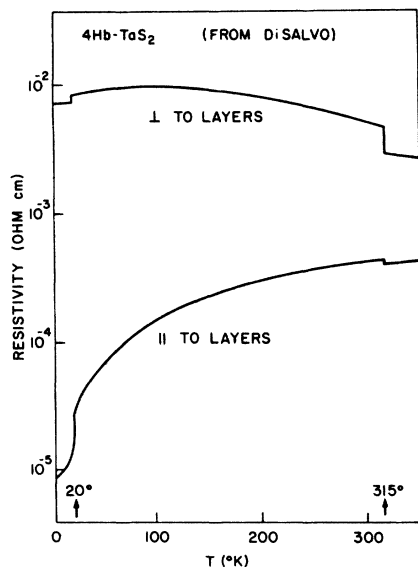
Earlier measurements of ΔH at 120 K in $2H$ - $TaSe_2$ by Bagley, reported in Ref. 1, give a value much lower than that reported here. It has been determined that this earlier measurement was unreliable at these temperatures, thus there is no disagreement with the present values.

Magnetic susceptibility measurements show a 20% decrease below T_0 suggesting a somewhat larger fraction of Fermi surface is involved than in $2H$ - TaS_2 .

D. $4Hb$ - TaS_2

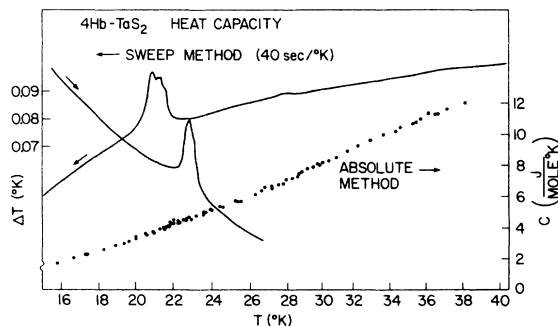
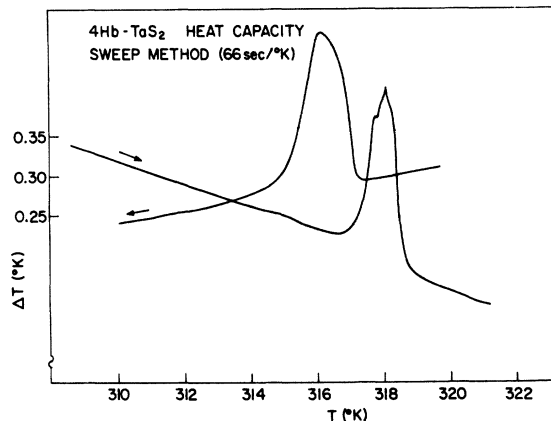
The $4Hb$ structure consists of alternate layers of octahedral and trigonal prismatic coordination. Electron-diffraction results^{1,29} and transport measurements⁶ show that the two types of layers behave quite independently in the establishment of CDW distortions. In Fig. 12 the resistivity anomalies at 315 and 20 K in $4Hb$ - TaS_2 are shown.¹ At 315 K the resistivity rises abruptly on cooling, at the ICDW to CCDW transition of the octahedral layers. At 20 K the resistivity drops, at a transition in the trigonal prismatic layers. Recent electron-diffraction measurements by Narayan²⁹ show the 22-K transition to be to a commensurate CDW in the trigonal prismatic layers.

The heat-capacity results for $4Hb$ - TaS_2 were previously reported in Ref. 30. Figure 13 shows both the absolute and sweep measurements of heat capacity in the region of the low temperature transition. In the absolute measurements no anomalies were observed, indicating that this is not a smooth second-order transition. In the sweep method a latent heat was observed (exothermic on cooling) with a hysteresis of about 1–2 K. The transition appeared slightly narrower on heating. Also, repeatable small anomalies in the sweep traces were observed at 28 and 38 K. While not easily visible in Fig. 13, these small anomalies appeared in repeated sweeps. The entropy associ-

FIG. 12. 4Hb-TaS₂ resistivity (from DiSalvo Ref. 1).

ated with the 22-K transition is similar to the transitions in 2H-NbSe₂ and 2H-TaS₂ (Table I), but presumably occurs only in the trigonal prismatic layers, thus corresponding to twice the entropy change per layer. The small anomalies observed at 28 and 38 K may be caused by phase adjustments between CDW's in different layers, adjustments of the CDW in the octahedral layers, or possibly the onset temperature of the CDW with the 22-K transition being T_d , the lock-in temperature in the trigonal prismatic layers.

The transition at 317 K is shown in Fig. 14. These measurements were made by heating the block above room temperature while maintaining the calorimeter in an ice bath. Absolute measurements at this temperature are very slow due to the long thermal time constants, so only one absolute measurement was made at 300 K to approximately calibrate the sweep method. The sweep method

FIG. 13. 4Hb-TaS₂ heat capacity at CDW transition at 22 K—relaxation method and sweep method.FIG. 14. 4Hb-TaS₂ heat capacity at CDW transition at 317 K—sweep method.

gave reproducible results similar to the 22-K transition. A latent heat was observed, with a hysteresis of 1–2 K, the warming curve again appearing somewhat narrower. A small anomaly was observed at 315 K, again not clearly visible in Fig. 14 but reproducible in repeated sweeps. The accuracy of these measurements above room temperature is very approximate due to operating the calorimeter above its intended temperature range. Previous measurements by DiSalvo *et al.*⁶ are more accurate at this temperature, so the value for ΔH obtained in their measurements is given in Table I for reference. The magnitude of entropy change is comparable to the higher temperature transitions in the 1T polytypes,¹ consistent with this transition occurring only in the octahedral layers.

E. 4Hb-TaSe₂

Neutron-scattering studies of 4Hb-TaSe₂ by Moncton³¹ show that a CCDW exists in the octahedral layers and an ICDW in the trigonal prismatic layers at low temperatures. A broad shoulder in the resistivity at 75 K (see Ref. 31) is interpreted as the CDW transition in the trigonal prismatic layers. This is in contrast with 4Hb-TaS₂ where a well-defined first-order transition occurs to a CCDW in the trigonal prismatic layers.^{1,29} Sweep heat-capacity measurements were made in the region of 75 K, but no anomalies were observed to the level of $\Delta C/C = 0.5\%$. Thus the CDW transition appears broadened in temperature. It remains to be seen whether this is a sample-dependent behavior in 4Hb-TaSe₂.

F. 1T-VSe₂

1T-VSe₂ has a variety of anomalous properties at low temperatures which have been interpreted as

due to CDW transitions at $T_0 = 112$ K and $T_d = 80$ K.⁷ Sweep measurements were made on a 3-mg crystal, but no thermal anomaly was found to a level of $\Delta C/C = 1\%$.

IV. DISCUSSION

The heat-capacity measurements show the existence of thermal anomalies at the CDW transitions, consistent with thermodynamic models. The CDW transitions in $2H\text{-NbSe}_2$ at 33 K, $2H\text{-TaS}_2$ at 78 K, and $2H\text{-TaSe}_2$ at 120 K appear to be second order, with well-defined thermal anomalies (with no hysteresis). The transitions in $2H\text{-TaSe}_2$ at 90 K, and $4Hb\text{-TaS}_2$ at 22 and 315 K show hysteresis and appear to be first order.

The Landau theory developed by McMillan⁴ predicts the heat capacity behavior at the CDW transitions. Neglecting interlayer interactions the onset transition (normal to ICDW) is predicted to have a first-order component, although the sharpness of the transition will be smeared by impurity effects. Also the lock-in transition (ICDW to CCDW) is predicted to be first order, with the transition temperature T_d suppressed by impurities or disorder. However, the inclusion of interlayer Coulomb interactions causes the onset transition to be second order. McMillan later developed a more sophisticated nonlinear Landau model⁴ in which the lock-in transition is not first order, but a continuous defect-melting-type transition.

The second-order nature of the thermal anomalies at the onset transitions is thus consistent with non-negligible interlayer interactions. As the neutron studies by Moncton^{2,31} have shown, the relative phasing of CDW's in different layers adjusts to minimize the Coulomb interactions.

At the lock-in transition in $2H\text{-TaSe}_2$ the thermal anomaly is too small to resolve the shape, thus a direct comparison with McMillan's predicted shape⁴ cannot be made to resolve the nature of this transition. Recent measurements of the pressure

dependence of T_0 and T_d in $2H\text{-TaSe}_2$ by Chu *et al.*³² show that T_0 increases slightly under pressure while T_d is suppressed to 0 K at about 17 kbar. The authors conclude that interlayer coupling is important in stabilizing the CDW state in $2H\text{-TaSe}_2$.

In $4Hb\text{-TaS}_2$ the 22-K transition has an entropy change similar to the onset transitions in the $2H$ materials, supporting the interpretation that this transition occurs in the trigonal prismatic layers.^{1,29} This transition in $4Hb\text{-TaS}_2$ remains to be fully characterized by x-ray or neutron scattering. The 315-K transition has an entropy comparable to the first-order lock-in transitions in $1T$ materials, consistent with it occurring in the octahedral layers.

If we assume the band structures of the three $2H$ compounds to be identical, then within the BCS-like model ΔH would increase as T_0^2 . In that case ΔH for $2H\text{-TaS}_2$ is smaller by a factor of 3 to 5 than that calculated. Of course, such a simple expectation of identical band structures is unrealistic, but the results for ΔH are qualitatively consistent with this idea.

Finally, we comment on the shape of the heat capacity anomaly. As previously mentioned, the shape of the anomaly at T_0 is not consistent with the simple mean-field models.⁴ The data show a pronounced peak (at least for $2H\text{-TaSe}_2$ and $2H\text{-TaS}_2$), the origin of which is not yet known. We speculate that this peak may be associated with the sharp rise in δ , the deviation from commensurability,² as T approaches T_0 , and could be described in a more-detailed mean-field model. It also seems possible that the transition at T_0 may not be mean-field-like.

ACKNOWLEDGMENTS

We thank R. A. Craven for discussion of his results prior to publication. We also thank R. G. Young and G. R. Ierley for help in developing the heat-capacity apparatus.

*Research at Stanford was supported by the Air Force Office of Scientific Research, Air Force Systems Command, USAF, under Grant No. AFOSR 73-2435B. One of the authors (J.H.) acknowledges the support of IBM.

¹J. A. Wilson, F. J. DiSalvo, and S. Mahajan, *Adv. Phys.* **24**, 117 (1975); P. M. Williams, G. S. Parry, and C. B. Scruby, *Philos.-Mag.* **29**, 695 (1974).

²D. E. Moncton, J. D. Axe, and F. J. DiSalvo, *Phys. Rev. Lett.* **34**, 734 (1975).

³T. M. Rice and G. K. Scott, *Phys. Rev. Lett.* **35**, 120 (1975).

⁴W. L. McMillan, *Phys. Rev. B* **12**, 1187 (1975); **12**, 1197 (1975); R. N. Bhatt and W. L. McMillan, *Phys. Rev.*

B **12**, 2042 (1975); W. L. McMillan (unpublished).

⁵J. M. E. Harper, Ph.D. dissertation (Stanford University, 1975) (unpublished).

⁶F. J. DiSalvo, B. J. Bagley, J. M. Voorhoeve, and J. V. Waszczak, *J. Phys. Chem. Solids* **34**, 1357 (1973).

⁷A. H. Thompson and B. G. Silbernagel, *Bull. Am. Phys. Soc.* **21**, 260 (1976); A. H. Thompson (private communication).

⁸F. J. DiSalvo, G. W. Hull, L. H. Schwartz, J. M. Voorhoeve, and J. V. Waszczak, *J. Chem. Phys.* **59**, 1922 (1973); F. R. Gamble, J. H. Osiecki, and F. J. DiSalvo, *J. Chem. Phys.* **55**, 3525 (1971).

⁹Wakefield Engineering, Inc., Wakefield, Mass.

¹⁰Model Cr-1000, Cryocal, Inc., Riviera Beach, Fla.

- ¹¹Model DT-500 P/GR, Lakeshore Cryogenics, Eden, N. Y.
- ¹²R. E. Schwall, R. E. Howard and G. R. Stewart, *Rev. Sci. Instrum.* **46**, 77 (1975).
- ¹³Model 124, Princeton Applied Research, Inc., Princeton, N. J.
- ¹⁴R. Bachmann, F. J. DiSalvo, T. H. Geballe, R. L. Greene, R. E. Howard, C. N. King, H. C. Kirsch, K. N. Lee, R. E. Schwall, H.-U. Thomas, and R. B. Zubeck, *Rev. Sci. Instrum.* **43**, 205 (1972).
- ¹⁵R. E. Schwall, Ph.D. dissertation (Stanford University, 1973) (unpublished).
- ¹⁶J. F. Revelli, Jr., Ph.D. dissertation (Stanford University, 1973) (unpublished).
- ¹⁷S. F. Meyer, Ph.D. dissertation (Stanford University, 1974) (unpublished).
- ¹⁸D. W. Murphy, F. J. DiSalvo, G. W. Hull, J. V. Waszczak, S. F. Meyer, G. R. Stewart, S. Early, J. V. Acrivos, and T. H. Geballe, *J. Chem. Phys.* **62**, 967 (1975).
- ¹⁹F. J. DiSalvo, *Ferroelectrics* (to be published).
- ²⁰R. C. Morris, *Phys. Rev. Lett.* **34**, 1164 (1975); C. Berthier, P. Molinie, and D. Jerome, *Solid State Commun.* **18**, 1393 (1976); C. W. Chu, V. Diatschenko, C. Y. Huang, and F. J. DiSalvo (unpublished).
- ²¹J. M. E. Harper, T. H. Geballe, and F. J. DiSalvo, *Phys. Lett. A* **54**, 27 (1975).
- ²²A. J. Bevolo and H. R. Shanks, *J. Appl. Phys.* **45**, 4644 (1974); and (unpublished).
- ²³M. Barmatz, L. R. Testardi, and F. J. DiSalvo, *Phys. Rev. B* **12**, 4367 (1975).
- ²⁴J. P. Tidman, O. Singh, A. E. Curzon, and R. F. Frindt, *Philos. Mag.* **30**, 1191 (1974).
- ²⁵R. A. Craven and S. F. Meyer (unpublished).
- ²⁶R. Delaplace, P. Molinie, and D. Jerome (unpublished).
- ²⁷M. Barmatz, L. R. Testardi, and F. J. DiSalvo, *Phys. Rev. B* **13**, 4637 (1976).
- ²⁸A. S. Barker, J. A. Ditzenberger, and F. J. DiSalvo, *Phys. Rev. B* **12**, 2049 (1975).
- ²⁹J. Narayan, *Appl. Phys. Lett.* **29**, 223 (1976).
- ³⁰J. M. E. Harper, T. H. Geballe, and F. J. DiSalvo, *Bull. Am. Phys. Soc.* **21**, 260 (1976).
- ³¹D. E. Moncton, *Bull. Am. Phys. Soc.* **21**, 362 (1976); F. J. DiSalvo, D. E. Moncton, J. A. Wilson, and S. Mahajan, *Phys. Rev. B* **14**, 1543 (1976).
- ³²C. W. Chu, L. R. Testardi, F. J. DiSalvo, and D. E. Moncton, *Phys. Rev. B* (to be published).